Pure & Appl. Chem., Vol. 61, No. 12, pp. 2117–2128, 1989.
Printed in Great Britain.

Electronic states and magnetic circular dichroism of cyclic π systems with antiaromatic perimeters

Udo Höweler, Prabir S. Chatterjee, Kenneth A. Klingensmith, Jacek Waluk, and Josef Michl

Center for Structure and Reactivity, Department of Chemistry, The University of Texas at Austin, Austin, Texas 78712-1167 U.S.A.[1]

Abstract: An analogue of the Moffitt - Platt perimeter model suitable for use with π systems derived from the antiaromatic 4*N*-electron perimeters has been developed. It yields a semiquantitative understanding of the electronic nature of the first few excited singlet states of hydrocarbons, heterocycles, and their substituted derivatives, a nomenclature analogous to but distinct from the familiar Platt-Moffitt L_b, L_a, B_b, B_a labeling of the states of aromatics, and a set of general simple rules for absorption intensities and MCD signs as a function of hydrocarbon topology and of the location and nature of perturbing heteroatoms and substituents. The results are illustrated by application to [3.3.3]cyclazine and to derivatives of pentalene and heptalene. Some cyclic π-systems, such as acenaphthylene and pleiadiene, can be derived from either a 4*N*- or a (4*N*+2)-electron perimeter. For these, either nomenclature can be used and the two sets of rules for MCD signs agree.

INTRODUCTION

Because of its simplicity and fundamental physical soundness, the perimeter model introduced by Platt (ref. 2) and Moffitt (ref.3) for polyacenes, extended later to azulenes (ref. 4) and porphyrins (ref. 5), and more recently generalized (ref. 6) to all π systems derivable from a (4*N*+2)-electron perimeter and to magnetic circular dichroism (MCD) in addition to ordinary and polarized absorption, has been very useful for the understanding of trends in the electronic spectra of aromatics as well as signs of bands in their MCD spectra. The Platt state notation, L_b, L_a, B_b, and B_a, or L_1, L_2, B_1, B_2 for charged perimeters (ref. 6), represents a valuable complement to the group theoretical notation, since it transcends an enormous diversity of structural variations.

For some time, the need has been felt (ref. 7) to devise a similar system of classification and back-of-the-envelope spectral prediction for π systems derived from 4*N*-electron perimeters, which represent a second huge class of spectroscopically interesting hydrocarbons, heterocyclics, and substituted derivatives, formally related to aromatics by the loss or the acquisition of two electrons. While some of these can equally well be derived from a (4*N*+2)-electron perimeter, most of them cannot (Fig. 1), and the Platt-Moffitt nomenclature and rules for absorption and MCD properties (ref. 6) are then not applicable. In the following, we describe a Platt-Moffitt-like model for π systems derived from a 4*N*-electron perimeter and illustrate its utility and generality on a few absorption and MCD spectra.

The spectroscopic observables of interest are the transition energy $W(F) - W(G)$, dipole strength D, polarization direction **u** for non-degenerate transitions, and the A, B, and C terms in MCD. Using $\hat{\mathbf{M}}$ for the electric dipole and $\hat{\boldsymbol{\mathcal{M}}}$ for the magnetic dipole operator, *G* for the ground, *F* for the final, and *K* for an arbitrary electronic state of energy $W(K)$, α for the degenerate components of the *F* state, κ for those of the *K* state, and γ for those of a *g*-fold degenerate *G* state, these are given in the usual approximation by

$$D = (1/g) \sum_{\alpha\gamma} |\langle F_\alpha|\hat{\mathbf{M}}|G_\gamma\rangle|^2$$

$$\mathbf{u} = \langle F|\hat{\mathbf{M}}|G\rangle / |\langle F|\hat{\mathbf{M}}|G\rangle|$$

$$A = (1/2g) \sum_{\alpha\gamma} (\langle F_\alpha|\hat{\boldsymbol{\mathcal{M}}}|F_\alpha\rangle - \langle G_\gamma|\hat{\boldsymbol{\mathcal{M}}}|G_\gamma\rangle) \cdot \mathrm{Im}(\langle G_\gamma|\hat{\mathbf{M}}|F_\alpha\rangle \times \langle F_\alpha|\hat{\mathbf{M}}|G_\gamma\rangle)$$

$$B = (1/g) \sum_{\alpha\gamma} \mathrm{Im}\Big(\sum_{\substack{K\kappa \\ K\neq F}} \langle F_\alpha|\hat{\boldsymbol{\mathcal{M}}}|K_\kappa\rangle \cdot \langle G_\gamma|\hat{\mathbf{M}}|F_\alpha\rangle \times \langle K_\kappa|\hat{\mathbf{M}}|G_\gamma\rangle [W(K) - W(F)]^{-1} + \sum_{\substack{K\kappa \\ K\neq G}} \langle K_\kappa|\hat{\boldsymbol{\mathcal{M}}}|G_\gamma\rangle \cdot \langle G_\gamma|\hat{\mathbf{M}}|F_\alpha\rangle \times \langle F_\alpha|\hat{\mathbf{M}}|K_\kappa\rangle [W(K) - W(G)]^{-1}\Big)$$

$$C = (1/2g) \sum_{\alpha\gamma} \langle G_\gamma|\hat{\boldsymbol{\mathcal{M}}}|G_\gamma\rangle \cdot \mathrm{Im}(\langle G_\gamma|\hat{\mathbf{M}}|F_\alpha\rangle \times \langle F_\alpha|\hat{\mathbf{M}}|G_\gamma\rangle)$$

where the summations run over all electronic states except as indicated. The quantity -2A/D is referred to as the magnetic moment of the excited state. Magnetically induced molar ellipticity per gauss is given by

$$[\Theta]_M = -21.34[f_2B + f_2(C/kT) + f_1A]$$

where f_2 is an absorption line shape, f_1 is its derivative, k is Boltzmann's constant and T is absolute temperature (ref. 8). It is important to note that the definition of the B term of a transition is such that this quantity is negative for peaks that appear with positive intensity in the MCD spectrum and positive for those MCD peaks that are negative in the spectrum.

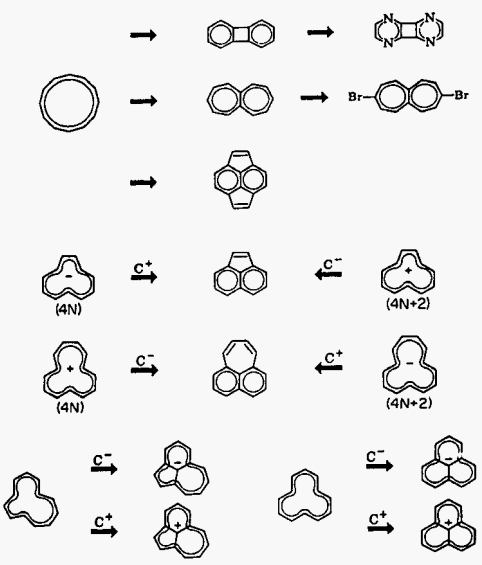

Fig. 1. Perturbation of $4N$-electron perimeters.

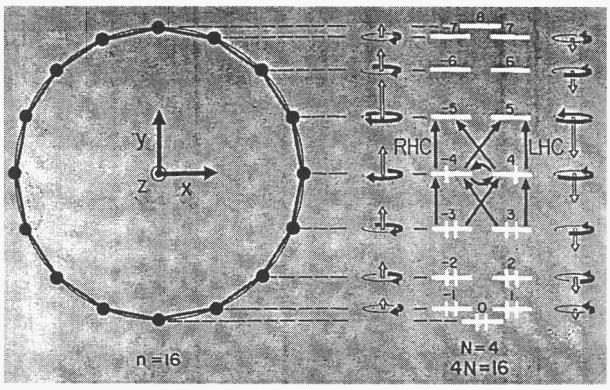

Fig. 2. Example of a C_n-symmetry [n]annulene (n=16) and the energies of its MO's, labelled by k. The net electron circulation in each MO and its magnetic moment are indicated. Electron occupancy in the Ψ_0 configuration of $C_{16}H_{16}$ (N=4), and the ten excitations involving HOMO (k = ± 3), SOMO (k = ± 4), and LUMO (k = ± 5) and included in the CI procedure are also shown.

PARENT 4N-ELECTRON [n]ANNULENES

The construction of the model and derivation of the results (ref. 9) follow closely those described for (4N+2)-electron systems (ref. 6, Fig. 2). A set of n $2p_z$ orbitals situated at the n vertices of a regular polygon located in the x,y plane is explicitly Löwdin-orthogonalized through second order in overlap and combined into n complex molecular orbitals ψ_k, $k = 0, \pm 1, \pm 2, \ldots$, by adaptation to C_n symmetry (k is the subscript on the label of the irreducible representation in the C_n group). These are doubly degenerate except for the lowest-energy one, ψ_0, and if n is even, the highest-energy one, $\psi_{n/2}$. The reference configuration Ψ_0 is constructed by using the $4N$ electrons to occupy doubly all orbitals up to the degenerate HOMO pair ψ_{N-1} and ψ_{-N+1}, and to occupy singly the members of the degenerate SOMO pair ψ_N and ψ_{-N}. The degenerate orbital pair ψ_{N+1} and ψ_{-N-1} represents the LUMO. Ten additional configurations are constructed by considering all single HOMO to SOMO, SOMO to SOMO, and SOMO to LUMO excitations. All higher configurations are ignored as being too high in energy; in addition, they carry no oscillator strength from the ground state. The zero-differential-overlap (ZDO) approximation is used to evaluate electron repulsions and a block-diagonal 11×11 CI matrix is formulated. Its exact form depends on the relation between n and N. Several special cases need to be distinguished and shall be fully considered elsewhere (ref. 9). We illustrate the results on the case $n = 4N$ ($N > 1$), i.e., on uncharged perimeters carrying eight, twelve, sixteen, etc., $2p_z$ AO's.

For these the ϵ_{2N} and ϵ_{-2N} representations of the C_n group coincide and are labeled b; the full symmetry of the polygon is D_{nh}. In this case, the CI matrix is

ϵ_0	Ψ_0	: [2N]	$s^*\sqrt{2}$	$s\sqrt{2}$	0	0	0	0	0	0	0	0
ϵ_{2N}	Ψ_{-N}^{N}	: $s\sqrt{2}$	0	[2N]	0	0	0	0	0	0	0	0
ϵ_{-2N}	Ψ_{N}^{-N}	: $s^*\sqrt{2}$	[2N]	0	0	0	0	0	0	0	0	0
ϵ_1	Ψ_{N}^{N+1}	: 0	0	0	c+[2N+1] -ΔHSL/4	-[1]	0	0	*l*	0	s^*	0
ϵ_1	Ψ_{N-1}^{N}	: 0	0	0	-[1]	c+[2N-1] +ΔHSL/4	0	0	0	$-h^*$	0	-*s*
ϵ_{-1}	Ψ_{-N}^{-N-1}	: 0	0	0	0	0	c+[2N+1] -ΔHSL/4	-[1]	*s*	0	l^*	0
ϵ_{-1}	Ψ_{-N+1}^{-N}	: 0	0	0	0	0	-[1]	c+[2N-1] +ΔHSL/4	0	$-s^*$	0	-*h*
ϵ_{-2N-1}	Ψ_{N}^{-N-1}	: 0	0	0	l^*	0	s^*	0	c+[1] -ΔHSL/4	-[2N-1]	0	0
ϵ_{2N-1}	Ψ_{-N+1}^{N}	: 0	0	0	0	-*h*	0	-*s*	-[2N-1]	c+[1] +ΔHSL/4	0	0
ϵ_{2N+1}	Ψ_{-N}^{N+1}	: 0	0	0	*s*	0	*l*	0	0	0	c+[1] -ΔHSL/4	-[2N-1]
ϵ_{-2N+1}	Ψ_{N-1}^{-N}	: 0	0	0	0	$-s^*$	0	$-h^*$	0	0	-[2N-1]	c+[1] +ΔHSL/4

where

$c = [E(L) - E(H)]/2 + [1] - [2N]$
$\Delta HSL = 2(\Delta HS - \Delta SL)$
$\Delta HS = E(S) - E(H)$
$\Delta SL = E(L) - E(S)$

Here, $E(H)$, $E(S)$, and $E(L)$ are the one-electron parts of the energies of the HOMO, SOMO, and LUMO orbital pairs, respectively, the quantities h, s, and l are equal to zero, and the two-electron integrals $[l]$ are defined by

$$[l] = \iint \psi_i^*(1)\psi_j(1)(e^2/r_{12})\psi_m^*(2)\psi_n(2)d\tau_1 d\tau_2$$

where $l = |i - j| = |m - n|$. One finds $[0] > [1] > [2] > \ldots > [2N]$. For the common values of n, $[2N]$ equals about 1 eV. Because of its simple form, the CI matrix can be diagonalized algebraically and explicit expressions for the state wave functions and their energies are obtained in all cases (ref. 9). In our case, $n = 4N$, the CI matrix is simplified in that ΔHSL vanishes.

Substitution of the eigenfunctions into the above expressions for spectroscopic observables yields their values in algebraic form as a function of the matrix elements of the one-electron operators for the electric ($\hat{\mathfrak{m}}$) and magnetic ($\hat{\mu}$) dipole moments over the complex MO's, which are known (ref. 6) trigonometric functions of n, N, the bond length, and the resonance integral. Of the former elements, only those containing orbitals whose "quantum numbers" k differ by one, $\langle\psi_k|\hat{\mathfrak{m}}|\psi_{k\pm1}\rangle$, do not vanish. Their absolute value is labeled $m(n,|2k \pm 1|)$. They mediate the absorption of a left-handed circularly polarized photon propagating along z upon promotion of an electron from ψ_k to ψ_{k+1} ($k > 0$) and of a right-handed circularly polarized one upon promotion from ψ_k to ψ_{k-1} ($k < 0$). Of the latter elements, only the diagonal ones, $\langle\psi_k|\hat{\mu}|\psi_k\rangle$, do not vanish. Their absolute value is labeled $-\mu(n,k)$; they are directed along z if $k < 0$ and along $-z$ if $k > 0$. Their relative magnitudes are shown in Fig. 2 along with a schematic indication of the net circular motion of an electron in the respective complex MO.

It is useful to define the quantities m_+ and μ_+ as the sums and m_- and μ_- as the differences of the HOMO and the LUMO orbital contributions to these moments:

$$m_\pm = |\langle\psi_N|\hat{\mathfrak{m}}|\psi_{N+1}\rangle| \pm |\langle\psi_N|\hat{\mathfrak{m}}|\psi_{N-1}\rangle| = m(n,2N+1) \pm m(n,2N-1)$$

$$\mu_\pm = -(|\langle\psi_{N+1}|\hat{\mu}|\psi_{N+1}\rangle| \pm |\langle\psi_{N-1}|\hat{\mu}|\psi_{N-1}\rangle|) = \mu(n,N+1) \pm \mu(n,N-1)$$

The sums are large, m_+ positive and μ_+ negative, while the differences are small. For an uncharged perimeter, m_- vanishes exactly within the model adopted here, and μ_- vanishes unless interactions between non-neighbors are included in the evaluation. These quantities are analogous to, but not identical with, the $m^\pm$ and $\mu^\pm$ terms familiar from the case of $(4N+2)$-electron perimeters (ref. 6).

Returning to our illustrative example $n = 4N$ ["pair biradicals" (ref. 10)], we see that the two low-energy SOMO to SOMO excited configurations are coupled in the CI matrix by the off-diagonal element $[2N]$. Their out-of-phase combination is stabilized by $[2N]$ and represents the lowest singlet state G (degenerate with the lowest triplet state in this approximation, in better approximations slightly below it). The in-phase combination is destabilized by the same amount and together with Ψ_0 forms the first excited singlet state (exactly degenerate in the ZDO approximation). The full symmetries of these three low-energy states are B_{1g}^-, B_{2g}^+, and A_{1g}^-. Transitions from the B_{1g}^- ground state into both others are forbidden. These results are well known (refs. 10,11).

All four higher excited states that result from the CI procedure when $N > 1$ are doubly degenerate. In increasing energy order, their symmetries are E^{+}_{1u}, $E^{-}_{2N+1,u}$, $E^{+}_{2N+1,u}$, and E^{-}_{1u}. Transitions from the B^{-}_{1g} ground state into the first and the last of these are forbidden, transitions into the second is weakly and into the third strongly allowed [$D = m_{-}^2$ and m_{+}^2, respectively; m_{-} vanishes in the usual PPP (ref. 12) approximation]. The MCD A terms are $-\mu_{-}m_{-}^2/4$ for the second and $-\mu_{-}m_{+}^2/4$ for the third transition. The B terms are

$$-2m_{-}m_{+}(\mu(n,N)[W(A_{1g}) - W(B_{1g})]^{-1} \pm (1/4)[\mu_{+} + 2\mu(n,N)][W(E^{-}_{2N+1}) - W(E^{+}_{2N+1})]^{-1})$$

where the plus sign applies for the second and the minus sign for the third transition. The C terms of both transitions vanish since the ground state is non-degenerate. When $N = 1$ (square cyclobutadiene), the number of states is reduced since HOMO and LUMO are both non-degenerate. Only two degenerate higher excited states remain, E^{-}_{1u} and E^{+}_{1u} in the order of increasing energy, with vanishing A, B, and C terms ($D = m_{-}^2$ and m_{+}^2, respectively).

For charged perimeters, $n \neq 4N$ ["axial biradical" (ref. 10)], the [$2N$] and [$2N$-1] off-diagonal matrix elements in the above CI matrix are missing. Instead, the matrix contains other off-diagonal elements containing two-electron integrals at other locations. Its exact form is a function of the difference between n and $4N$ and also depends on the number of orbitals in the HOMO and LUMO sets. This may be less than two in each when n is small, and then the size of the CI matrix is less than 11×11 so that fewer states result, as outlined above for cyclobutadiene.

In the case of charged perimeters, ΔHSL does not vanish: it is positive for anionic perimeters and negative for cationic ones. The ground state is doubly degenerate (E_{2N}) and consists of the two SOMO to SOMO promoted configurations (refs. 10,11). The reference configuration Ψ_0 represents the next higher state, which carries no oscillator nor MCD strength. A series of allowed and forbidden excited states then follows at higher energies and simple expressions for their spectroscopic properties can be written (ref. 9).

The results for the perfectly symmetrical parent $4N$-electron perimeters are of limited practical interest since [$4N$]annulenes are subject to Jahn-Teller or pseudo-Jahn-Teller distortions and do not have C_n symmetry in reality; only a few are known. What makes these results useful is that they provide a starting point for the introduction of perturbations that convert the parent perimeters into π systems of real interest (Fig. 1).

PERTURBED 4N-ELECTRON [n]ANNULENES

Typical perturbations needed to convert an idealized perimeter into a model of a real molecule are a variation of bond lengths, introduction of new π bonds by transannular interaction, by σ cross-links, by bridging across the perimeter through additional conjugating groups, or by introduction of substituents, and modification of AO electronegativity by introduction of heteroatoms. All these changes are modelled by one-electron operators $\hat{a}$. At the orbital level, we assume that these operators only cause mixing of complex MO's that are degenerate. At the CI level, their effect is also simple. The diagonal elements of the perturbed CI matrix differ from those of the original matrix in that the energy of the reference configuration, the value of c, and the value of ΔHSL have changed in ways that are easily estimated from first-order perturbation theory, and new off-diagonal elements are introduced. These are the quantities h, s, and l given in the above example of a CI matrix, which now no longer need to vanish. These complex CI matrix elements are equal to the matrix elements of the perturbing one-electron operator $\hat{a}$ between the members of the HOMO, SOMO, and LUMO orbital pairs, respectively:

$$h = \langle\psi_{N-1}|\hat{a}|\psi_{-N+1}\rangle = e^{i\eta}\Delta H/2$$
$$s = \langle\psi_{N}|\hat{a}|\psi_{-N}\rangle = e^{i\sigma}\Delta S/2$$
$$l = \langle\psi_{N+1}|\hat{a}|\psi_{-N-1}\rangle = e^{i\lambda}\Delta L/2$$

They are just the elements responsible for the lifting of the degeneracy of the HOMO, SOMO, and LUMO orbital levels, by amounts equal to ΔH, ΔS, and ΔL, respectively. Since we neglect the mixing of non-degenerate MO's by the perturbing operator $\hat{a}$, ΔH, ΔS, and ΔL are identical with the orbital energy differences in the perturbed system. Estimates of their values are generally available, from experiments, from calculations of various types, or from first-order perturbation theory [PMO (ref. 13)]. The phase angles η, σ, and λ are related to the angle of complex rotation needed to make the sum and the difference of ψ_k and ψ_{-k} real, with $k = N$-1, N, and N+1, respectively. The real orbitals are defined by

$$h_{\pm} = (\psi_{N-1}e^{i\eta/2} \pm \psi_{-N+1}e^{-i\eta/2})/\sqrt{2}$$
$$s_{\pm} = (\psi_{N}e^{i\sigma/2} \pm \psi_{-N}e^{-i\sigma/2})/\sqrt{2}$$
$$l_{\pm} = (\psi_{N+1}e^{i\lambda/2} \pm \psi_{-N-1}e^{-i\lambda/2})/\sqrt{2}$$

where the phase angles are always chosen so that orbital k_{-} is of lower energy than k_{+}, $k = h,s,l$. The phase angles account for the adjustment of positions of the nodes and antinodes

in the real MO's to the symmetry that remains after the perturbation. If the molecule contains a mirror plane perpendicular to the molecular plane, all three phase angles η, σ, and λ are equal to integral multiples of $\pi/2$. In this important case, an algebraic solution of the CI problem is possible as described below, and explicit expressions for the spectroscopic observables can be obtained.

There are two classes of perimeter perturbations. The first comprises high-symmetry perturbations that either preserve the C_n symmetry available in the perimeter, or reduce it to $C_{n/m}$, where $n/m > 2$, and produce either perfect biradicals ($\Delta S = 0$) or biradicaloids ($\Delta S \neq 0$). Examples of the latter are the C_8H_8, $C_{12}H_{12}^{4+}$, $C_{12}H_{12}^{4-}$, and $C_{16}H_{16}$ perimeters perturbed to fourfold symmetry, $C_9H_9^{3-}$, $C_{12}H_{12}$, $C_{15}H_{15}^{3+}$, and $C_{15}H_{15}^{9-}$ perimeters perturbed to threefold symmetry, the $C_{12}H_{12}$ perimeter perturbed to sixfold, or the $C_{15}H_{15}^{5-}$ perimeter perturbed to fivefold symmetry. The second class comprises low-symmetry perturbations, for which none of the perimeter orbitals remain degenerate and $\Delta S \neq 0$. These always produce biradicaloids. If the perturbation is strong enough and the separation of the frontier orbitals, ΔS, large enough, the biradicaloids in effect are quite ordinary closed-shell molecules (we shall keep the label biradicaloid for simplicity and to trace their lineage within our model). In these, the ground state will be well approximated by a closed-shell configuration in which the real MO's h_-, h_+, and s_- are all doubly occupied while s_+, l_-, and l_+ are empty. This reference configuration will be labeled Ψ_R and others will be referred to it in obvious notation such as $\Psi_{s_+}^{s_-}$ and $\Psi_{s_+;s_+}^{s_-;s_-}$ for single and double excitation from s_- to s_+. The configurations built from the real orbitals span the same many-electron space as those built from the complex MO's that we have dealt with so far but are more appropriate for the perturbed systems with $\Delta S \neq 0$. We adopt them in the following.

While it is obvious how a perturbation acts on a one-electron level, producing a finite gap between the frontier orbitals s_- and s_+, its action on the total many-electron wavefunctions is more complicated. First, we need to consider the way in which the perturbation converts the ground-state wavefunction $(\psi_{-N}^N - \psi_N^{-N})/\sqrt{2}$ of an uncharged perimeter, and ψ_N^{-N}, ψ_{-N}^N (degenerate) for a charged one, into the Ψ_R wavefunction of the ground state of a very strongly perturbed system. As described in more detail elsewhere (ref. 10), all three low-energy configurations, Ψ_R, $\Psi_{s_+}^{s_-}$, and $\Psi_{s_+;s_+}^{s_-;s_-}$ must be considered simultaneously.

The results depend on the value of σ. For any value of σ in a charged perimeter, and for $\sigma = \pi/2$ in an uncharged perimeter, the weight of Ψ_R in the ground state wavefunction changes gradually as the strength of the perturbation ΔS increases and equals $\cos^2\alpha$, where $\alpha = (1/2)\tan^{-1}([2N]/\Delta S)$ in an uncharged and $\alpha = (1/2)\tan^{-1}([2N]/2\Delta S)$ in a charged perimeter ["homosymmetric biradicaloid" (ref. 10)]. In an uncharged perimeter with $\sigma = 0$, the change is abrupt: the weight of Ψ_R in the lowest singlet state is zero as long as $\Delta S < 2[2N]$, and unity if $\Delta S > 2[2N]$ ["heterosymmetric biradicaloid" (ref. 10)]. At $\Delta S = 2[2N]$, the ground state is degenerate, with Ψ_R as one of the components. In an uncharged perimeter with other values of σ ["non-symmetric biradicaloid" (ref. 10)], the expression for the weight of Ψ_R is more complicated. The results are represented graphically in Fig. 3. For instance, when $\Delta S = 2[2N]$, the weight of Ψ_R in the ground state is 95% in an uncharged and 98.5% in a charged perimeter. For three important cases the energies of the three lowest singlets are shown as a function of the perturbation strength ΔS in Fig. 4.

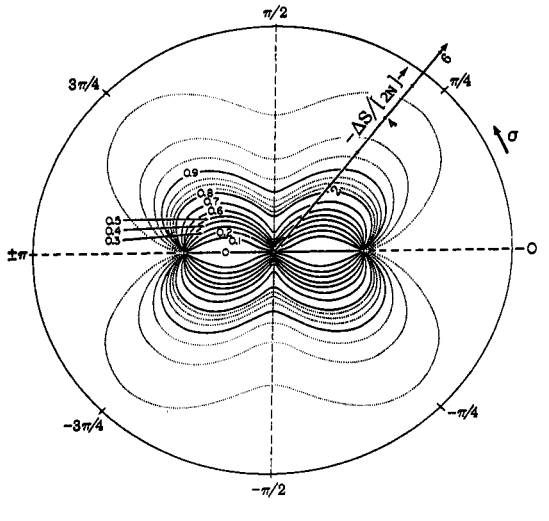

Fig. 3. A contour diagram showing the weight of Ψ_R in the ground state of a high-symmetry biradicaloid derived from an uncharged perimeter as a function of σ and ΔS in units of $[2N]$.

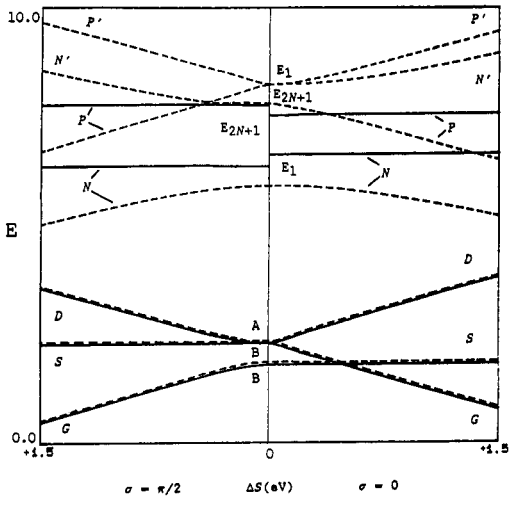

Fig. 5. Energies of singlet states as a function of ΔS in the 7×7 (full) and 11×11 (dashed) CI approximation.

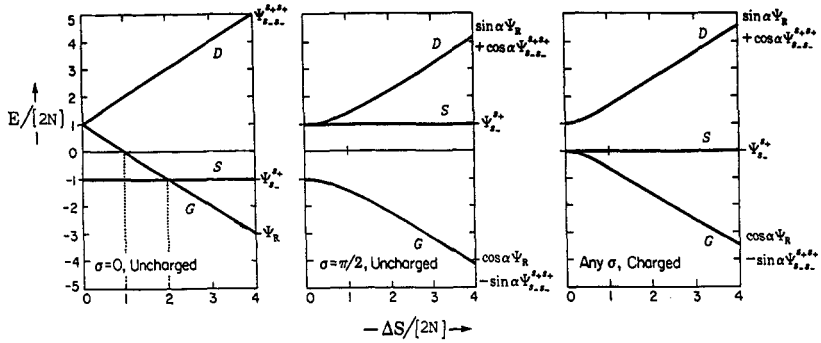

Fig. 4. Energies of the lowest three singlet states of high-symmetry biradicaloids as a function of ΔS in units of $[2N]$.

It is clear from the above and from Fig. 3 that Ψ_R is a good approximation to the ground state wave function as soon as the perturbation ΔS causes a significant splitting of the s_- and s_+ orbitals, certainly when it exceeds $2[2N]$. This is virtually guaranteed for all systems of real interest even if no structural perturbations are present, due to Jahn-Teller and pseudo-Jahn-Teller distortions. In the following, we assume that such is the case and that the wave function of the ground state is Ψ_R.

This, in turn, suggests that it should be reasonable to reduce the dimensionality of the CI space under consideration from 11×11 to 7×7 when dealing with perturbed 4N-electron annulenes of practical interest. In addition to the three low-energy configurations discussed so far, Ψ_R, Ψ^S_{S+}, and $\Psi^{S,S}_{S+,S+}$, we include the four configurations resulting from Ψ_R upon single excitation from s_- into l_- or l_+ and from h_- or h_+ into s_+. These are just the configurations adopted by Wirz in his discussion of excited states of molecules derived from antiaromatic perimeters (ref. 7). The four configurations that are left out of consideration are doubly excited with respect to Ψ_R.

HIGH-SYMMETRY PERTURBATIONS

In the 7×7 CI approximation, the case $\Delta S \neq 0$, $\Delta H = \Delta L = 0$, has a simple explicit solution for the wave functions and spectroscopic observables in the case of all charged perturbed perimeters as well as those uncharged perimeters for which $\sigma = 0$ or $\pi/2$. The energies obtained in the 7×7 and in the 11×11 CI approximations are compared in Fig. 5. The two sets of results are identical for the lowest three singlets, labeled G, S (for singly excited), and D (for doubly excited) in the order of increasing energy and dominated by Ψ_R, Ψ^S_{S+}, and $\Psi^{S,S}_{S+,S+}$, respectively. For the next two states the energies obtained at the 7×7 level are a little higher than those at the 11×11 level, but the wave functions are very similar in both approximations. Each of these states is doubly degenerate; the lower is labeled N (for negative) and the upper P (for positive; the origin of this designation will become clear below). In the 11×11 CI treatment, two additional doubly degenerate states are present at still higher energies, labelled N' and P'. These cannot be described in the 7×7 CI approximation, but anyway are at such high energies that they are not normally observed and that the use of the simple perimeter model would be questionable. For the G, S, D, N, and P states the 7×7 CI model should be adequate and offers the important advantage of simplicity and of access to algebraic solutions, which permit the formulation of general qualitative rules (ref. 9). We use it in the following.

Fig. 5 shows how the states of a high-symmetry perturbed biradicaloid relate to those of an unperturbed uncharged parent perimeter in the cases $\sigma = 0$ and $\pi/2$. For other values of σ, the crossings are avoided and it is clear that there is no unique general relation between the B^-, B^+, A, E^+_1, and E^-_{2N+1} states of the unperturbed and the G, S, D, N, and P states of the perturbed perimeter. This is quite different from the classical case of $(4N+2)$-electron perimeters, whose electronic states correlate simply with those of their perturbed derivatives regardless of the nature of the perturbation, providing the basis for Platt and Moffitt's state nomenclature (refs. 2,3). In the present case of $4N$-electron perimeters, the group theoretical labels are best used for the states of the parent perimeters and the G, S, D, N, and P labels for the perturbed derivatives.

The algebraic results for the spectroscopic transitions in a high-symmetry biradicaloid are quite simple (ref. 9). Transitions into the low-energy S and D states are forbidden within the model. In reality, they must be expected to acquire some weak absorption and MCD intensity, at least by vibronic borrowing, but the sign of the resulting weak MCD intensity cannot be predicted at the present level of approximation, since it considers electronic terms only.

The dipole strengths of the transitions into the symmetry-allowed isotropically in-plane polarized degenerate states N and P are

$$D(N) = (m_+\sin\beta + m_-\cos\beta)^2$$
$$D(P) = (m_+\cos\beta - m_-\sin\beta)^2$$
$$-\pi/4 \leq \beta \leq \pi/4$$

Here, $\beta = (1/2)\tan^{-1}([\Delta HSL/2 + ([2N\text{-}1]\text{-}[2N\text{+}1])^{\ddagger}]/([1] \pm [2N\text{-}1]^{\dagger})$, where the plus sign holds for $\sigma = \pi/2$ and the minus sign for $\sigma = 0$, and where the terms labeled with a dagger are absent unless the perimeter is uncharged and those labeled with a double dagger are absent unless it is charged. The expressions for the MCD A terms are

$$-2A(N)/D(N) = (\mu_- + \mu_+\sin 2\beta)/2$$
$$-2A(P)/D(P) = (\mu_- - \mu_+\sin 2\beta)/2$$

The expressions for the B terms are more complicated but still permit simple sign predictions by inspection (ref. 9).

Once the perimeter is defined by specifying its size and charge, i.e., n and N, the only unknown that remains to be specified before the dipole strengths and the A terms can be predicted is ΔHSL, and this is determined by the nature of the perturbation in a straightforward way. Its sign determines the sign of β and thus the signs of A and B terms of the N and P transitions. We have already noted that in the unperturbed systems ΔHSL is positive in anionic perimeters, negative in cationic perimeters, and zero in uncharged perimeters. First-order perturbation theory is normally sufficient to predict the sign and estimate the magnitude of ΔHSL in the actual molecule of interest. This is particularly simple when ΔHSL vanishes to start with, since then, the perturbation alone determines the resulting sign. For this reason, we refer to uncharged perimeters and other high-symmetry systems with vanishing ΔHSL as "soft" MCD chromophores: their MCD signs are easily modified and are dictated already by weakly interacting substituents, heteroatoms, etc. Charged perimeters and more complicated high-symmetry systems with ΔHSL very different from zero are referred to as "hard" MCD chromophores. Their MCD signs are intrinsic in that they are difficult to change by structural perturbations. High-symmetry MCD chromophores with positive ΔHSL are called positive-hard, those with negative ΔHSL, negative-hard. The concepts of soft and hard MCD chromophores are already familiar from the treatment of π systems derived from $(4N+2)$-electron perimeters where they are dictated by the value of ΔHOMO-ΔLUMO (ref. 6). Now, we generalize them to those derived from $4N$-electron perimeters, at first, high-symmetry ones. Below, we shall generalize them further to include chromophores of low symmetry.

The way in which ΔHSL dictates the MCD signs is through controlling the value of β. This vanishes when ΔHSL vanishes [for charged perimeters, the controlling quantity is $\Delta HSL + 2([2N\text{-}1] - [2N\text{+}1])$, which is almost the same]. Then, inspection of the algebraic expressions for the spectroscopic observables shows that the transition into the N state has very small (in uncharged perimeters, zero) absorption intensity and that the P transition has high intensity. This mutual cancellation of orbital contributions to the transition moment of the lower symmetry-allowed transition and their mutual reinforcement in the case of the upper one have inspired the labels N and P for negative and positive interference, respectively.

The magnetic moments of the N and P states are both equal to $\mu_-/2$. Because of the difference in dipole strengths, N is expected to have a weakly and P a more strongly positive A term.

When ΔHSL or its equivalent for charged perimeters is positive, so is β. Then, the N transition acquires some intensity at the expense of the P transition, the A and B terms for the former are more strongly positive, and those for the latter less strongly positive or negative. The MCD sign predictions for the N transition are thus unambiguous: positive A and B terms. Those for the P transition are less clear-cut: when ΔHSL is weakly positive, the positive contribution from the μ_- term may still dominate. For strongly positive ΔHSL, the negative contribution from μ_+ should prevail. A similar situation is familiar from the $(4N+2)$-electron perimeter series (ref. 6). Finally, when ΔHSL or its equivalent is negative, so is β, transition intensity is again distributed from P to N, but the changes in the MCD terms are just the opposite. Now, the prediction of positive A and B terms for the P transition is unambiguous while the MCD signs for the N transition may be in doubt. In a sense, the absorption spectra of systems with a positive and those with a negative ΔHSL are alike, while their MCD spectra are approximate mirror images of each other.

In summary, we find that for high-symmetry systems derived from $4N$-electron perimeters, the energy ordering of the excited configurations determines the MCD signs. If the configurations that describe HOMO to SOMO excitations are higher in energy than those that describe SOMO to LUMO excitations, the A and B terms for the N transition are positive and those for the P transition are negative, whereas the opposite signs result if the ordering of the configurations is reversed.

[3.3.3]Cyclazine. This molecule has been chosen as an illustration of the high-symmetry case. It can be derived from [12]annulene by union with a methyl anion bridge, which reduces the symmetry to D_{3h} and introduces $\Delta HSL > 0$, and replacement of the central carbon by a nitrogen. Fig. 6 shows the relevant orbitals and their SCF energies in the PPP approximation. The even simpler Hückel approximation would actually be more appropriate to represent the one-electron energies but both do equally well for our purposes. Either way, it is clear that the phenalenide anion and the derived heterocycle have a positive ΔHSL and are positive-hard MCD chromophores, whereas the corresponding phenalenyl cation would have a negative one and should be a negative-hard one.

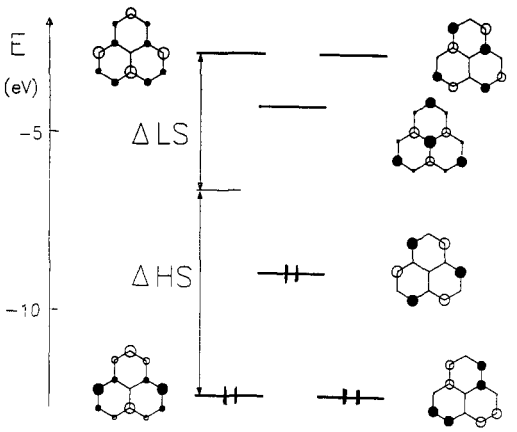

Fig. 6. Frontier orbitals of [3.3.3]-cyclazine and their energies in the PPP approximation.

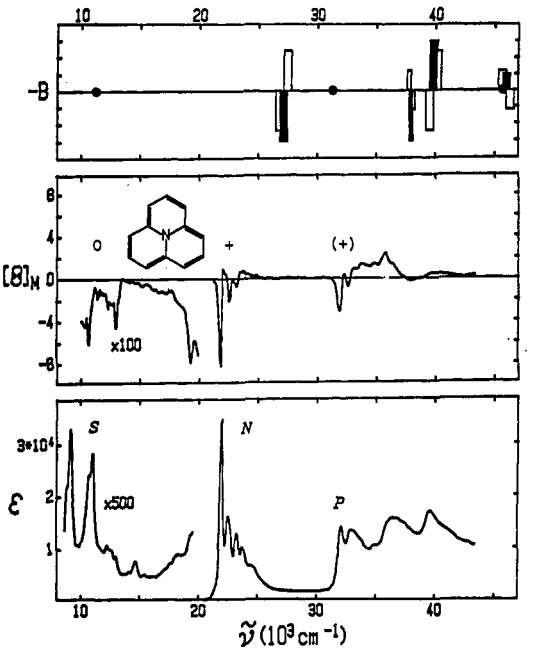

Fig. 7. Absorption (bottom) and MCD (center) spectra of [3.3.3]cyclazine. Top, PPP calculation: dots, symmetry-forbidden transitions, white bars, A terms; black bars, B terms.

The observed absorption and MCD spectra (ref. 14) of [3.3.3]cyclazine (Fig. 7) indeed show a weak transition near 10 000 cm^{-1} assigned as the forbidden *S* band, presumably observable only because of vibronic borrowing, and neglected in the present model. This is followed by an intense band at 22 000 cm^{-1}, with positive A and B terms, assigned to the *N* transition, and an intense band at 33 000 cm^{-1}, with weaker positive A and B terms, assigned to the *P* transition. The MCD observations for the *N* transition agree well with expectations. The observed A and B terms of the *P* transition are less positive, as expected, and their sign suggests that ΔHSL in this molecule is not large enough for the μ_+ term to dominate. This is somewhat surprising and disagrees with the numerical calculations by the PPP method, which are also shown in Figure 7. This is not so for all symmetrical [3.3.3]cyclazine derivatives in that in some cases the A and B terms of the high-energy *P* transition are negative as expected. In general, we find flawless agreement at lower energies and occasional disagreement at higher ones, possibly due to magnetic mixing of the latter with higher energy states, not included in the model. The situation is quite reminiscent of that encountered (ref. 6) with $(4N+2)$-electron perimeters.

LOW-SYMMETRY PERTURBATIONS

In the general case of a perturbed $4N$-electron perimeter, not only ΔS but also ΔH and ΔL are different from zero (Fig. 8). The ordering of the configurations still is of paramount importance for the spectroscopic observables, but now is determined by three parameters, ΔHSL, ΔH, and ΔL, and the phase angles η, σ, and λ may all be different. The 7×7 CI problem is again soluble algebraically, provided that $\sigma - (\eta + \lambda)/2$, and for uncharged perimeters, also $\sigma + (\eta + \lambda)/2$, are equal to an integral multiple of $\pi/2$. This is the case in all molecules containing a plane of symmetry perpendicular to the molecular plane.

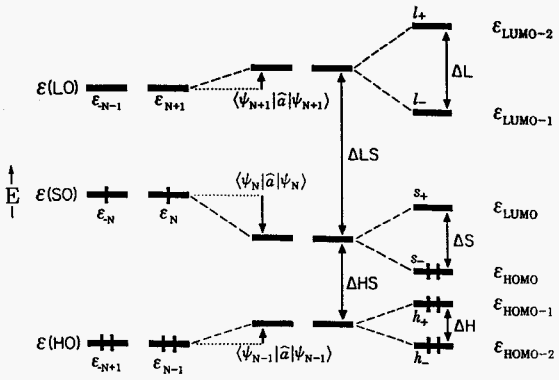

Fig. 8. Orbital energies of a low-symmetry perturbed $4N$-electron perimeter.

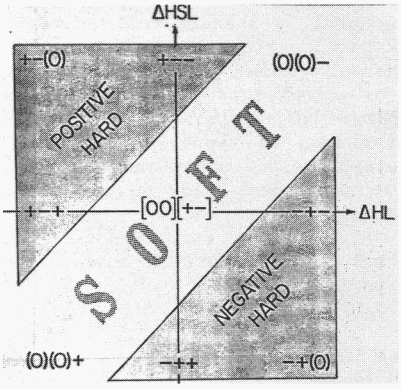

Fig. 9. Signs of the B terms of the N_1, N_2, and P_1 transitions in a perturbed $4N$-electron perimeter as a function of ΔHSL and ΔHL and a classification of chromophores. Signs combined in brackets represent those of the two peaks of an A term in the order of increasing energy. B terms that vanish in the first approximation are placed in parentheses.

In the general case, the ground state G and six excited states result, since all degeneracies are now removed. In an obvious extension of the notation we have just introduced, they shall be labeled S, D, N_1, N_2, P_1, and P_2. A terms now vanish but additional contributions to the B terms are present, due to the mutual magnetic mixing within the no longer degenerate N_1, N_2, and P_1, P_2 state pairs. The dipole strength for the transitions into the N_1, N_2, P_1, and P_2 states is distributed between the two members of each pair and remains smaller for both N states than it is for the two P states.

There are two limiting cases: in orbital-shift dominated systems, $|\Delta HSL| > |\Delta H + \Delta L|$ and in orbital-splitting dominated ones, $|\Delta HSL| < |\Delta HL|$. In the former, the N and P state pairs are well separated in energy from one another. Then, the mutual magnetic mixing within these pairs will dictate the signs of their B terms. In the latter, this will still be so for the N_1 and P_2 transitions, but not for N_2 and P_1, which are close in energy so that their B terms are determined by their mutual magnetic mixing. The intermediate case, $|\Delta HL| \leq |\Delta HSL| \leq |\Delta H + \Delta L|$, is more complicated but can be analyzed as well (ref. 9).

One now also needs to consider the effects of the magnetic mixing of the S state into the ground state G, which no longer vanish. Their signs are positive for the two states dominated by the SOMO to LUMO configurations and negative for the two dominated by the HOMO to SOMO configurations.

The algebraic expressions for the spectroscopic observables are relatively complicated and will be given elsewhere (ref. 9). The transitions to the S and D states are still forbidden, as they were in the high-symmetry case. The general features of the results for the signs of the B terms of the N_1, N_2, and P_1 transitions as a function of ΔHSL and ΔHL are summarized in Fig. 9. The result for the high-energy P_2 transition are not considered reliable because of the likely magnetic mixing with even higher-energy states, not included in the model.

Fig. 9 makes it clear that the MCD intensity of the N_1 and N_2 transitions will be small or zero for molecules in which ΔHSL and ΔHL are approximately equal. These are soft MCD chromophores, and the high-symmetry case considered earlier was merely a special case, in which ΔHSL and ΔHL were both equal to zero. In positive-hard chromophores, $\Delta HSL > \Delta HL$, and the signs of the B terms expected for the N_1 and N_2 transitions are positive and negative, respectively. The expectations for the sign of the B term of the P_1 transition depend on the absolute values of ΔHSL and ΔHL. If the former is larger, this sign is negative, if the latter is larger (orbital-splitting dominated systems), the sign is positive. In negative-hard chromophores, $\Delta HSL < \Delta HL$, and the signs expected for all three transitions are just the opposite of those described above for positive-hard chromophores. Once again, the previously considered case of high symmetry represents merely a special case. Introduction of substituents and other perturbations that affect ΔHSL and/or ΔHL are not expected to change the MCD signs of hard chromophores, unless their effect is unusually strong, and are expected to dictate the MCD signs of soft chromophores.

In general, π systems derived from negatively charged $4N$-electron perimeters by relatively weak perturbations tend to have positive ΔHSL, and they usually are positive-hard MCD chromophores. Those derived from positively charged $4N$-electron perimeters by relatively weak perturbations tend to have negative ΔHSL and usually are negative-hard, those derived from uncharged $4N$-electron perimeters by weak perturbations tend to have small ΔHSL and have the best chance to represent soft MCD chromophores. Of course, in many actual molecules of interest the perturbation is so strong that they do not follow these simple generalizations, as we shall see below on the examples of pentalene, heptalene, acenaphthylene, and pleiadiene.

Systems that are derived from $4N$-electron perimeters that have a reduced number of states in the perimeter model, $C_3H_3^-$, C_4H_4, $C_5H_5^+$, $C_6H_6^{2+}$, $C_6H_6^{2-}$, $C_nH_n^{n-4}$ ($N = 1$), $C_nH_n^{4-n}$ ($N = n/2 - 1$), and $C_nH_n^{2-n}$ [$N = (n - 1)/2$], require a separate treatment using the same general principles.

It is interesting to note that the mirror-image symmetry between positive-hard and negative-hard chromophores derived from uncharged perimeters is related to their alternant pairing properties. By a general theorem (ref. 15), two π systems related by alternant pairing have identical absorption and mirror-image MCD spectra in the usual PPP approximation in which only nearest-neighbor resonance integrals are considered. Examples are naphthalene radical cation and naphthalene radical anion, or naphthalene dication and naphthalene dianion. A π system paired with itself, such as naphthalene, therefore has a vanishing MCD spectrum in this approximation and is a soft MCD chromophore.

In the usual PPP approximation, two π systems derived from an uncharged $4N$-electron perimeter and related by alternant pairing have identical ΔS, ΔHS of one equals ΔSL of the other, and ΔH of one equals ΔL of the other. As a result, their ΔHSL values are equal in magnitude and opposite in sign, as are their ΔHL values, and the above stated rules for MCD signs are compatible with the general theorem. An example that we have already encountered is the phenalenyl cation - anion pair. If a system derived from an uncharged $4N$-electron perimeter is alternant-paired with itself (an uncharged alternant hydrocarbon, such as biphenylene), its ΔHSL as well as ΔHL vanish in the usual PPP approximation, and so should its MCD spectrum - it should be a soft chromophore.

When non-nearest-neighbor interactions are introduced, the alternant pairing properties hold only approximately, and so do the mirror-image properties predicted for MCD. MCD spectroscopy indeed represents an excellent tool for the detection of the shortcomings of the usual PPP model. In alternant hydrocarbons containing four-membered conjugated rings, such as biphenylene, there is a quite significant resonance integral across the square diagonal that in effect makes the π system nonalternant and ΔHSL positive. This is clearly reflected in its MCD spectrum (ref. 16).

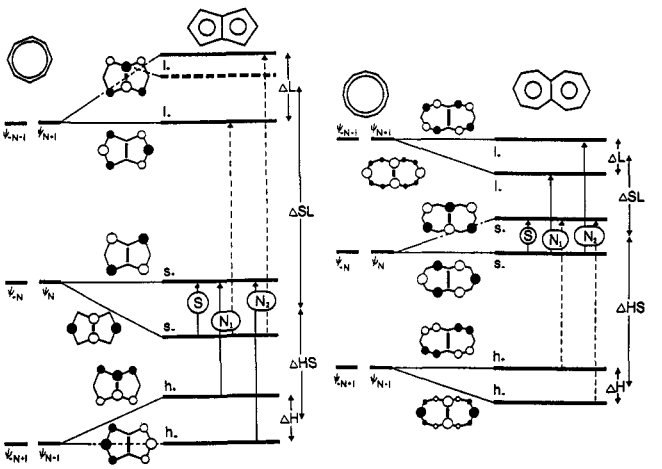

Fig. 10. Derivation of the MO energy diagrams of pentalene (left) and heptalene (right) using PMO theory.

Pentalene and heptalene. A symmetrical introduction of a single cross-link across an uncharged $4N$-electron perimeter has easily predictable consequences. First-order perturbation theory (Fig. 10) leads to the conclusion that the resulting bicyclic system is orbital-shift dominated: ΔHL will be small and ΔHSL large. It also shows that the sign of the latter will be positive when N is odd and negative when it is even. Pentalene ($N = 2$) should therefore be a negative-hard and heptalene ($N = 3$) a positive-hard MCD chromophore. We find that simple derivatives of these unstable hydrocarbons indeed have the expected MCD spectra (ref. 17). As shown in Fig. 11 on representative examples, the spectra of both types of compounds start with an extremely weak low-energy band assigned to the S transition, and at higher

energies contain two stronger bands attributed to the N_1 and N_2 transitions. The signs of their B terms are minus and plus, respectively, for the pentalene derivatives, and plus and minus, respectively, for the heptalene derivatives, as expected from the simple theory. The P_1 and P_2 transition occur at energies that are too high for reliable measurement on our instrument.

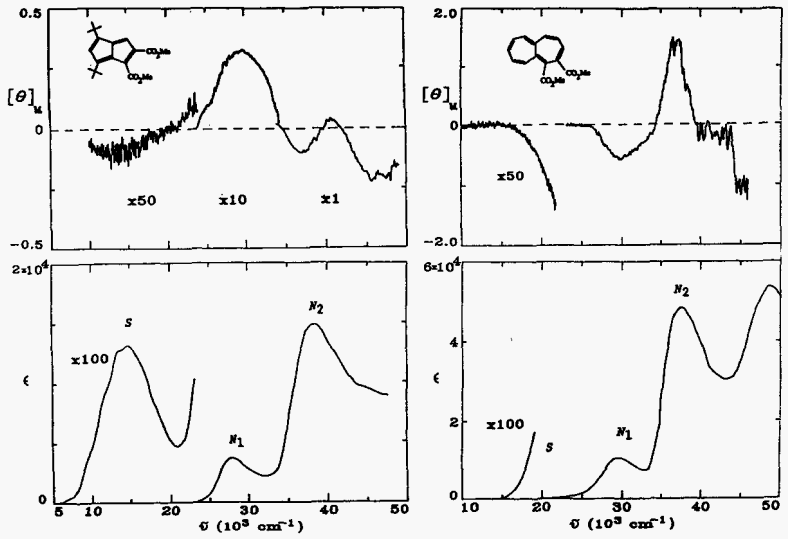

Fig. 11. Absorption (bottom) and MCD (top) spectra of derivatives of pentalene (left) and heptalene (right) (ref. 17).

Acenaphthylene and pleiadiene. These π systems can be formally derived from (4*N*+2)-electron perimeters by the union of the methyl anion with the [11]annulenyl cation to yield acenaphthylene, and by the union of the methyl cation with the [13]annulenyl anion to yield pleiadiene (ref. 18). In that case, the first transition must be considered as an intruder since it is not simply derived from the states of the unperturbed perimeter. Its properties do not follow from the Platt-Moffitt perimeter model (refs. 2,3,6). The signs of the B terms of the second (L_1) and third (L_2) transitions follow the standard rules for systems derived from (4*N*+2)-electron perimeters (ref. 18). In acenaphthylene, ΔHOMO < ΔLUMO, the chromophore is negative-hard, and the signs of the B terms are minus and plus, respectively. In pleiadiene, ΔHOMO > ΔLUMO, the chromophore is positive-hard, and the signs are plus and minus, respectively.

However, these two π systems may just as well be derived from 4*N*-electron perimeters. This ought to lead to a different nomenclature for their transitions, but hopefully to the same predictions for the spectral properties. This is indeed the case. As shown in Fig. 12, where acenaphthylene is derived from the methyl cation and the [11]annulenyl anion, and pleiadiene from the methyl anion and the [13]annulenyl cation, we have $\Delta HSL < 0$ for the former and $\Delta HSL > 0$ for the latter. The former is again negative-hard and the latter positive-hard. The first three transitions are now labeled *S*, N_1, and N_2, and the very weak intensity of the first one as well as the MCD signs of the latter two are accounted for by the perimeter model described presently.

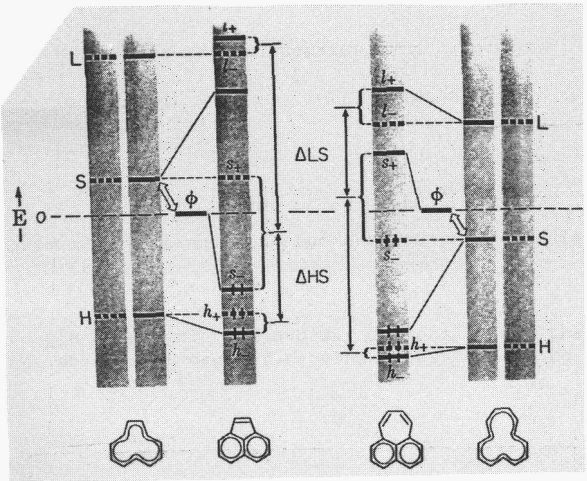

Fig. 12. Derivation of the MO energy diagrams of acenaphthylene (left) and pleiadiene (right) using PMO theory.

SUMMARY

π-Electron systems derived from $4N$-electron perimeters are amenable to a system of classification and spectral prediction quite analogous to that introduced by Platt and Moffitt for those derived from $(4N+2)$-electron perimeters. In particular, it is possible to predict the qualitative features of the absorption and MCD spectra by inspection of molecular structural formulas combined with the use of first-order perturbation theory, entirely without recourse to computations. It is hoped that this will facilitate the understanding of trends in the spectra of large groups of π-electron chromophores that have so far remained outside the realm of simple analysis.

Acknowledgement

This work was supported by the U.S. Public Health Service (NIH grant GM 37929). Udo Höweler is grateful to the Deutsche Forschungsgemeinschaft for a scholarship. We thank Prof. J. Wirz and Dr. W. Leupin for a kind gift of [3.3.3]cyclazine and Profs. K. Hafner and E. Vogel for kind gifts of pentalene and heptalene derivatives.

REFERENCES

1. The bulk of this project was performed while the authors were at the University of Utah.
2. J. R. Platt, *J. Chem. Phys.* **17**, 484 (1949).
3. W. Moffitt, *J. Chem. Phys.* **22**, 320 (1954); W. Moffitt, *J. Chem. Phys.* **22**, 1820 (1954).
4. E. Heilbronner and J. N. Murrell, *Mol. Phys.* **6**, 1 (1963).
5. M. Gouterman, *J. Mol. Spectrosc.* **6**, 138 (1961).
6. J. Michl, *J. Am. Chem. Soc.* **100**, 6801, 6812, 6819 (1978); J. Michl, *Tetrahedron* **40**, 3845 (1984).
7. J. Wirz, *Excited States in Organic Chemistry and Biochemistry*, B. Pullman and N. Goldblum, Eds., p. 283, Reidel, Dordrecht, Holland (1977).
8. P. N. Schatz and A. J. McCaffery, *Quart. Rev. Chem. Soc.* **23**, 552 (1969).
9. U. Höweler and J. Michl, to be published.
10. V. Bonačić-Koutecký, J. Koutecký and J. Michl, *Angew. Chem., Int. Ed. Engl.* **26**, 170 (1987).
11. L. Salem and C. Rowland, *Angew. Chem., Int. Ed. Engl.* **11**, 92 (1972); W. T. Borden, *Biradicals*, p. 1, W. T. Borden, Ed., Wiley, New York (1982).
12. R. Pariser and R. G. Parr, *J. Chem. Phys.* **21**, 466 (1953); J. A. Pople, *Trans. Faraday Soc.* **49**, 1375 (1953).
13. M. J. S. Dewar and R. C. Dougherty, *The PMO Theory of Organic Chemistry*, Plenum Press, New York (1975).
14. J. Waluk, P. S. Chatterjee, W. Leupin, J. Wirz and J. Michl, to be published.
15. J. Michl, *J. Chem. Phys.* **61**, 4270 (1974).
16. U. Höweler, J. Spanget-Larsen and J. Michl, to be published.
17. K. A. Klingensmith, U. Höweler, P. S. Chatterjee and J. Michl, to be published.
18. E. W. Thulstrup and J. Michl, *J. Am. Chem. Soc.* **98**, 4533 (1976); J. Kolc and J. Michl, *J. Am. Chem. Soc.* **98**, 4540 (1976); J. W. Kenney, III, D. A. Herold and J. Michl, *J. Am. Chem. Soc.* **100**, 6884 (1978).